AGU PUBLICATIONS

JGR

Journal of Geophysical Research: Earth Surface

RESEARCH ARTICLE
10.1002/2016JF004133

Key Points:
- We produced a year-round record of glacier velocity and surface elevation to investigate dynamic changes at Helheim and Kangerlussuaq
- Seasonal speedups and dynamic thinning occurred at both glaciers but through different processes
- Seasonal dynamic thinning altered the spatial extent of floating ice near the terminus, which affected iceberg-calving behavior

Supporting Information:
- Supporting Information S1
- Movie S1
- Movie S2

Correspondence to:
L. M. Kehrl,
kehrl@uw.edu

Citation:
Kehrl, L. M., I. Joughin, D. E. Shean, D. Floricioiu, and L. Krieger (2017), Seasonal and interannual variabilities in terminus position, glacier velocity, and surface elevation at Helheim and Kangerlussuaq Glaciers from 2008 to 2016, *J. Geophys. Res. Earth Surf.*, *122*, doi:10.1002/2016JF004133.

Received 4 NOV 2016
Accepted 15 AUG 2017
Accepted article online 17 AUG 2017

Seasonal and interannual variabilities in terminus position, glacier velocity, and surface elevation at Helheim and Kangerlussuaq Glaciers from 2008 to 2016

L. M. Kehrl[1,2], I. Joughin[1], D. E. Shean[1,3], D. Floricioiu[4], and L. Krieger[4]

[1]Polar Science Center, Applied Physics Lab, University of Washington, Seattle, Washington, USA, [2]Department of Earth and Space Sciences, University of Washington, Seattle, Washington, USA, [3]Department of Civil and Environmental Engineering, University of Washington, Seattle, Washington, USA, [4]Remote Sensing Technology Institute, German Aerospace Center (DLR), Wessling, Germany

Abstract The dynamic response of Greenland tidewater glaciers to oceanic and atmospheric change has varied both spatially and temporally. While some of this variability is likely related to regional climate signals, glacier geometry also appears to be important. In this study, we investigated the environmental and geometric controls on the seasonal and interannual evolution of Helheim and Kangerlussuaq Glaciers, Southeast Greenland, from 2008 to 2016, by combining year-round, satellite measurements of terminus position, glacier velocity, and surface elevation. While Helheim remained relatively stable with a lightly grounded terminus over this time period, Kangerlussuaq continued to lose mass as its grounding line retreated into deeper water. By summer 2011, Kangerlussuaq's grounding line had retreated into shallower water, and the glacier had an ~5 km long floating ice tongue. We also observed seasonal variations in surface velocity and elevation at both glaciers. At Helheim, seasonal speedups and dynamic thinning occurred in the late summer when the terminus was most retreated. At Kangerlussuaq, we observed summer speedups due to surface-melt-induced basal lubrication and winter speedups due to ice-shelf retreat. We suggest that Helheim and Kangerlussuaq behaved differently on a seasonal timescale due to differences in the spatial extent of floating ice near their termini, which affected iceberg-calving behavior. Given that seasonal speedups and dynamic thinning can alter this spatial extent, these variations may be important for understanding the long-term evolution of these and other Greenland tidewater glaciers.

1. Introduction

The contribution of the Greenland Ice Sheet to sea level rise more than quadrupled from 1991–2001 to 2002–2011 [*Shepherd et al*., 2012] as a result of enhanced surface melt and increased ice discharge from tidewater glaciers [*Enderlin et al*., 2014; *Van Den Broeke et al*., 2016]. While this widespread increase in ice discharge has been attributed, likely correctly, to ocean warming [*Holland et al*., 2008; *Hanna et al*., 2009; *Murray et al*., 2010; *Straneo et al*., 2010], there has been significant spatial variability in the dynamic response of individual glaciers [*Moon et al*., 2012]. Tidewater glaciers in the same fjord, which are likely subject to similar oceanic and atmospheric conditions, have behaved differently [*Rignot et al*., 2016; *Motyka et al*., 2017], indicating that individual glacier characteristics, such as glacier geometry, likely play an important role in modulating a glacier's dynamic response [*Enderlin et al*., 2013; *Amundson*, 2016; *Felikson et al*., 2017].

The dynamics of tidewater glaciers are sensitive to changes near the terminus [*Nick et al*., 2009]. Many Greenland tidewater glaciers have a grounded or nearly grounded terminus, and consequently, the terminus position often closely corresponds with the grounding-line position (location where the ice transitions from grounded to floating). Several processes have been proposed to link terminus retreat to oceanic and atmospheric changes, including enhanced submarine melt [*Holland et al*., 2008; *Motyka et al*., 2011], ice-mélange weakening [*Joughin et al*., 2008a; *Amundson et al*., 2010], and increased hydrofracture of water-filled crevasses [*Benn et al*., 2007]. Once retreat is initiated, the glacier's geometry will affect its dynamic response. Retreat into deeper water can promote speedup, thinning, and further retreat, whereas retreat into shallower water can cause the glacier to slow and to perhaps stabilize [*Meier and Post*, 1987; *Schoof*, 2007]. Furthermore, lateral constrictions in glacier width can help stabilize the terminus at a particular location [*Gudmundsson et al*., 2012]. As a result of these dynamic feedbacks, it can be difficult to attribute a change in glacier dynamics to a specific oceanic or atmospheric forcing.

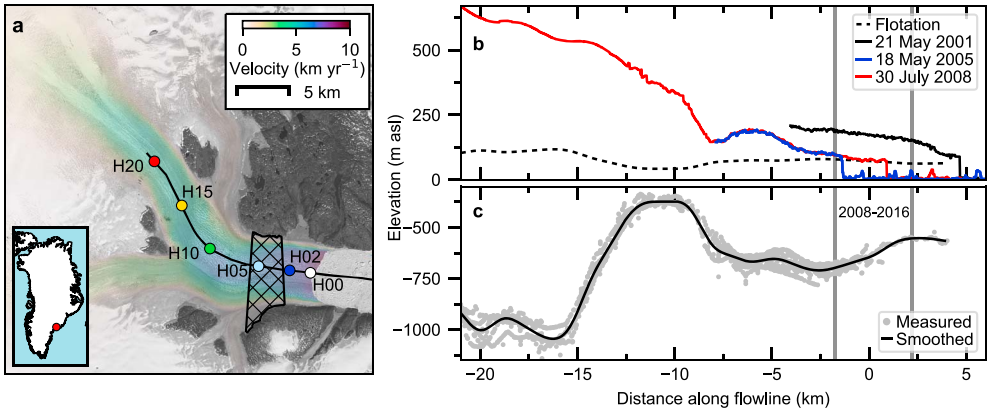

Figure 1. (a) Glacier velocity at Helheim from 30 June to 11 July 2014. Background image is the Landsat 8 panchromatic band from 4 July 2014. The colored circles indicate the locations of sample points plotted in Figure 3. Sample point names indicate the distance in kilometers from the mean terminus position from 2008 to 2016. We calculated surface-elevation change rates for the hatched region. Black curve indicates the profile shown in Figures 1b and 1c. (b) Glacier surface elevations from ATM. Black dashed line is the height where the ice should become afloat. (c) Smoothed bed elevations and all measured CreSIS bed elevations within 200 m of the profile. Gray vertical lines indicate the range of observed terminus positions from 2008 to 2016.

To address this difficulty, several studies have turned to seasonal records of terminus position [*Howat et al.*, 2010; *Seale et al.*, 2011; *Schild and Hamilton*, 2013] and glacier velocity [*Moon et al.*, 2014, 2015]. By comparing these records to different climatic variables over many years, these studies have attempted to correlate seasonal changes in terminus position and/or glacier velocity to oceanic and atmospheric changes. However, often there is no clear relationship between glacier dynamics and environmental change: the timing of the seasonal onset of retreat and speedup varies spatially from glacier to glacier and temporally from year to year at individual glaciers [*Schild and Hamilton*, 2013; *Moon et al.*, 2014]. Seasonal and multiyear variations in glacier geometry (ice thickness, surface slope, and grounding-line position) have been put forward as a possible mechanism to help explain this temporal variability at individual glaciers [e.g., *Schild and Hamilton*, 2013], but until recently, we have lacked the necessary seasonal surface-elevation records to explore this hypothesis further.

In this study, we combined year-round records of terminus position, glacier velocity, and surface elevation from 2008 to 2016 to investigate seasonal and multiyear changes in glacier geometry at Helheim and Kangerlussuaq Glaciers (Figures 1 and 2), the two largest tidewater glaciers in Southeast Greenland. Helheim and Kangerlussuaq collectively drain ~8% of the Greenland Ice Sheet area [*Nick et al.*, 2013]. Both glaciers rapidly retreated, accelerated, and thinned in the early 2000s [*Rignot et al.*, 2004; *Howat et al.*, 2005, 2007; *Stearns and Hamilton*, 2007]. The resulting dynamic mass loss from these two glaciers alone accounted for roughly 30% of the 2000–2012 dynamic mass loss from the entire Greenland Ice Sheet [*Enderlin et al.*, 2014]. After their retreats ended in 2006, both glaciers slowed, but Helheim stopped thinning while Kangerlussuaq continued thinning [*Howat et al.*, 2011; *Bevan et al.*, 2012]. The glaciers have also behaved differently on a seasonal timescale; terminus positions typically varied seasonally at Kangerlussuaq but showed little seasonality at Helheim [*Joughin et al.*, 2008b; *Schild and Hamilton*, 2013]. By comparing the varying evolution of Helheim and Kangerlussuaq over seasonal and multiyear timescales, we develop new insights into how differences in glacier geometry affect a glacier's dynamic response to oceanic and atmospheric changes. In particular, we focus our analysis on changes in the spatial extent of floating ice near the terminus, which can affect iceberg-calving behavior [*Benn et al.*, 2007].

2. Methods

We combined several different data sets to develop seasonal records of glacier velocity, terminus position, iceberg-calving behavior, surface elevation, and surface-elevation change rates at Helheim and Kangerlussuaq from 2008 to 2016. To interpret these observations, we also considered bed elevations, ice-mélange conditions, sea ice fraction (SIF), and modeled glacier surface runoff in our analysis.

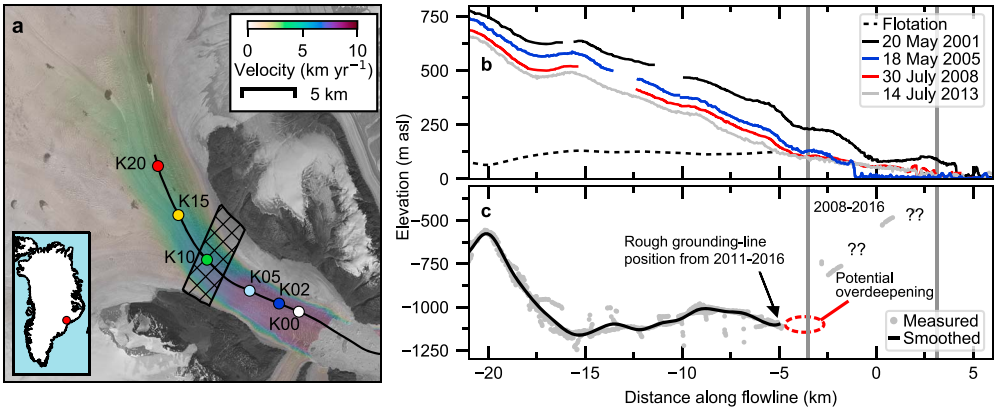

Figure 2. (a) Glacier velocity at Kangerlussuaq from 1 to 12 July 2014. The background image is the Landsat 8 panchromatic band from 6 July 2014. The colored circles indicate the locations of sample points plotted in Figure 6. We calculated surface-elevation change rates for the hatched region. Black curve indicates the profile shown in Figures 2b and 2c. (b and c) See Figure 1 for the descriptions. The black arrow indicates the approximate location of Kangerlussuaq's grounding line from 2011 to 2015, and the red ellipse indicates the location of a potential overdeepening discussed in the text. Bed elevations are very poorly constrained downstream of −5 km because the glacier was typically floating in this region when radar thicknesses were collected.

2.1. Glacier Velocity

To measure glacier velocity, we applied speckle tracking techniques [*Joughin*, 2002; *Joughin et al.*, 2010] to pairs of synthetic aperture radar (SAR) images from the German Aerospace Center's (DLR) TerraSAR-X (TSX) mission [*Krieger et al.*, 2013]. This satellite started acquiring data over Helheim and Kangerlussuaq in September 2008. A second, virtually identical satellite, TDX, was launched in June 2010 to complete the tandem configuration of the TanDEM-X (TDM) mission. The repeat period of each satellite allows velocity estimates to be determined over intervals as short as 11 days. Due to missed acquisitions, some velocity estimates were computed using 22 or 33 day intervals. We did not attempt estimates for intervals longer than 33 days, leaving some gaps in our record. All velocity estimates were smoothed with a moving average filter to a spatial resolution of ~300 m. Conversion from the radar line of sight to the horizontal across-track direction under a surface-parallel flow assumption can yield slope-dependent errors of up to 3% [*Joughin et al.*, 2010]. For observations collected along the same satellite track, this is a systematic error common to all estimates, so the error does not apply to changes in velocity. Of our 264 velocity products, 237 (90%) were collected along the same track for each glacier.

2.2. Terminus Position

We measured terminus position by digitizing the location where the calving front intersects the longitudinal profiles shown in Figures 1a and 2a. We chose this method over the box method [*Moon and Joughin*, 2008] because it allowed us to include satellite images with high cloud cover and Landsat 7 images with gaps due to the scan line corrector failure, which improved the temporal resolution of our records. Terminus positions were digitized in all available TSX/TDX radar images and Worldview-1/2/3 (WV) and Landsat 7/8 panchromatic scenes. We report terminus position relative to the 2008–2016 average, with a negative (positive) value indicating a more retreated (advanced) terminus position than average.

To assess uncertainties in the measured terminus positions, we compared digitized terminus positions from satellite images that were acquired on the same day when no large calving events occurred between the acquisitions. Consequently, the uncertainty estimates account for errors due to manual digitization and errors introduced by including satellite images with different spatial resolution, acquisition geometry, and spectral characteristics. The 22 pairs of coincident, digitized terminus positions differed by 2–42 m, with a root-mean-square (RMS) difference of 24 m.

2.3. Iceberg-Calving Behavior

We used the available satellite images to assess the calved iceberg type. Two types of icebergs have been observed previously at Helheim and Kangerlussuaq: tabular and nontabular [*Joughin et al.*, 2008b]. Tabular

icebergs have a large longitudinal width-to-height ratio and do not capsize when they calve. These icebergs can be distinguished in the satellite images by the presence of crevasses on their surfaces (Figure S1a in the supporting information). Nontabular icebergs capsize when they calve due to their smaller width-to-height ratio and greater buoyancy-driven torque (Figure S1b) [*Amundson et al*., 2010; *James et al*., 2014]. We compared subsequent satellite images to determine the type of new icebergs in the fjord after each iceberg-calving episode. We refer to periods of iceberg calving as "episodes" rather than as "events" because we cannot determine if the icebergs calved during a single event or during a series of events that occurred over several days.

Iceberg-calving episodes were divided into three types: (1) tabular, (2) nontabular, and (3) mixed (both tabular and nontabular). We considered an episode to be "tabular" if new tabular icebergs appeared in the fjord that could account for the observed retreat between subsequent satellites images. If new tabular icebergs appeared but could not account for all of the observed retreat, then the episode was considered "mixed." All other episodes were considered "nontabular." This approach may incorrectly characterize some tabular or mixed iceberg-calving episodes as nontabular if the tabular icebergs broke up and overturned between subsequent satellite images. However, the observed tabular icebergs typically remained intact for several weeks, suggesting that we observed a substantial fraction of tabular icebergs before they broke up.

2.4. Glacier Surface Elevation

We combined point surface-elevation measurements from NASA's Airborne Topographic Mapper (ATM) [*Krabill*, 2010] with digital elevation models (DEM) from WV, GeoEye-1, SPIRIT [*Korona et al*., 2009], and TanDEM-X (TDM). DEMs from WV and GeoEye-1 were created following the stereo-photogrammetry techniques outlined in *Shean et al*. [2016]. TDM DEMs were processed from bistatic SAR acquisitions using the Integrated TanDEM-X Processor [*Rossi et al*., 2012]. Large absolute elevation offsets in the resulting TDM DEMs are caused by baseline-dependent interferometric SAR (InSAR) height ambiguities and were corrected by adjusting the absolute phase offset during InSAR processing.

To reduce georeferencing errors, all DEMs were coregistered to ground control points (GCPs) over exposed rock. We adjusted the DEMs using a rigid-body translation that minimized the elevation difference between the DEMs and the GCPs [*Shean et al*., 2016]. All available ICESat-1 data [*Zwally et al*., 2003], LVIS data [*Blair and Hofton*, 2010], and ATM data over exposed bedrock surfaces were included as GCPs. After coregistration, the uncertainty of each DEM was estimated using the normalized median absolute deviation (NMAD) [*Höhle and Höhle*, 2009] of all GCP-DEM differences [*Shean et al*., 2016]. The average NMADs for the WV and TDM DEMs were 1.18 m and 1.77 m, respectively.

2.5. Bed Elevation and Flotation Condition

While several gridded bed-elevation products exist for Helheim and Kangerlussuaq [e.g., *Bamber et al*., 2013; *Morlighem et al*., 2014], there are large discrepancies among these products due to different interpolation methods. Consequently, to avoid errors introduced by interpolation, we used bed-elevation point measurements from the Helheim and Kangerlussuaq 2006–2014 Composite V3 products from the Center for Remote Sensing of Ice Sheets (CReSIS). We also included the CReSIS radar transect from 21 May 2001 in our analysis for Helheim.

Some of the radar thicknesses in the Composite V3 products were collected over floating ice. To determine if a radar thickness was collected over floating ice, we used the ATM surface-elevation measurements that were collected concurrently with the radar-thickness measurements. If the measured surface elevation was less than or equal to the flotation height for a given radar thickness (assuming an ice density of 917 kg m^{-3} and seawater density of 1025 kg m^{-3}), then we considered the ice at that location to be floating and removed that measurement from our analysis of bed elevations. Almost all radar thicknesses acquired over the lower 5 km of Kangerlussuaq were collected over floating ice (Figure 2c). After removing these points, the RMS for the bed-elevation crossover differences in regions below sea level improved from 113 m to 45 m for Helheim and from 90 m to 44 m for Kangerlussuaq. Given that crossover differences were $<$50 m for 80% of the crossovers, we assumed a bed-elevation uncertainty of 50 m.

We used the bed-elevation measurements, along with the available surface-elevation measurements, to calculate the spatial extent of floating and grounded ice for each glacier. In particular, we focused our analysis on determining regions where the ice remained "grounded" or "floating" or switched between grounded and

floating ("changing") from 2011 to 2015. We characterized a point as "grounded" ("floating") if its surface elevation remained more than 5 m above (below) the flotation threshold from 2011 to 2015. The 5 m cutoff accounts for bed-elevation uncertainties of 50 m and surface-elevation variations due to tides [*Voytenko et al.*, 2015]. All other points are characterized as likely "changing" between grounded and floating. (Note that the large-scale spatial patterns discussed in the text are unaffected by changing this 5 m cutoff within a reasonable range of 0–10 m.)

2.6. Surface-Elevation Change Rate

To better understand the observed variations in glacier surface elevation, we calculated the average rate of elevation change for the hatched regions in Figures 1a and 2a using two different methods: (1) we differenced all pairs of DEMs with time intervals of less than 4 months, and (2) we used the surface velocity and elevation measurements to estimate the ice flux in and out of the region. We refer to these methods as the "DEM" and "fluxgate" methods, respectively. While the DEM method provides more accurate estimates of the surface-elevation change rate, the fluxgate method increases the temporal resolution of our records from every few months (when we have DEMs) to every few weeks (when we have surface velocities) and also provides insight into the causes of the observed elevation changes. In the fluxgate method, we assumed that the rate of surface-elevation change (dh/dt) averaged over the region equaled the rate of ice-thickness change (dH/dt), which we calculated as

$$\frac{dh}{dt} = \frac{dH}{dt} = \frac{1}{A}\left[\int_0^{W_i} u_i(x,t)H_i(x,t)dx - \int_0^{W_o} u_o(x,t)H_o(x,t)dx\right] + \dot{a}, \quad (1)$$

where A is the area of the region, t is time, x is the coordinate parallel to the inflow or outflow boundary, $H(x,t)$ is the ice thickness at the boundary, $u(x,t)$ is the glacier velocity normal to the boundary, W is the glacier width at the boundary, and $\dot{a}$ is the elevation change rate due to surface mass balance (assuming basal melt is negligible). The subscripts signify values at the inflow (i) and outflow (o) boundaries. We calculated dh/dt for all time periods with surface-velocity measurements and linearly interpolated the surface-elevation measurements to match those time periods. To estimate $\dot{a}$, we used surface mass balance from the nearest grid cell in the 11 km resolution Regional Atmospheric Climate Model version 2.3 (RACMO2.3) [*van Angelen et al.*, 2013; *Noël et al.*, 2015] and assumed a constant density (900 kg m^{-3}) to convert surface mass balance to an elevation change rate.

Several key assumptions and measurement errors contributed to uncertainties in the inferred dh/dt from the fluxgate method. First, we assumed that the depth-averaged velocity was equal to the measured surface velocity (equation (1)). Although this is only an approximation, basal sliding accounts for >90% of the surface velocity under the main trunk of Helheim and Kangerlussuaq [*Shapero et al.*, 2016], so the depth-averaged velocity should be within ~2% of the surface velocity [*Cuffey and Paterson*, 2010]. This approximation contributed to uncertainties in dh/dt of <1 cm d^{-1}. Second, we assumed that basal melt is negligible. While there are currently no direct measurements of basal melt beneath the grounded portions of these or other tidewater glaciers, the melt rate should be <3 cm d^{-1} based on theoretical calculations (Text S1 in the supporting information) [*Cuffey and Paterson*, 2010]. Third, bed-elevation errors of 50 m could introduce systematic errors in dh/dt of >30 cm d^{-1}. To mitigate this error, we positioned the boundaries of the hatched regions in Figures 1a and 2a along CreSIS radar transects that had distinct bed returns and low bed-elevation crossover differences. Fourth, the RACMO surface mass balance product likely introduced additional uncertainties [*Noël et al.*, 2016]; however, these uncertainties are difficult to quantify given the limited surface-mass balance measurements collected over Helheim and Kangerlussuaq [*Andersen et al.*, 2010]. Finally, errors in the surface elevation and velocity measurements introduced random errors in dh/dt of ~3 cm d^{-1}.

To determine an error estimate that incorporated all of the above sources of uncertainty, we compared the surface-elevation change rates from the fluxgate and DEM methods. Although the surface-elevation change rates calculated using the two methods are not directly comparable due to differences in temporal resolution, comparing the two methods does provide an upper bound on the uncertainty in the rates inferred from the fluxgate method. The RMS difference between dh/dt calculated using the two methods was 3 cm d^{-1} for Helheim and 5 cm d^{-1} for Kangerlussuaq (Text S2 and Figures S2–S4).

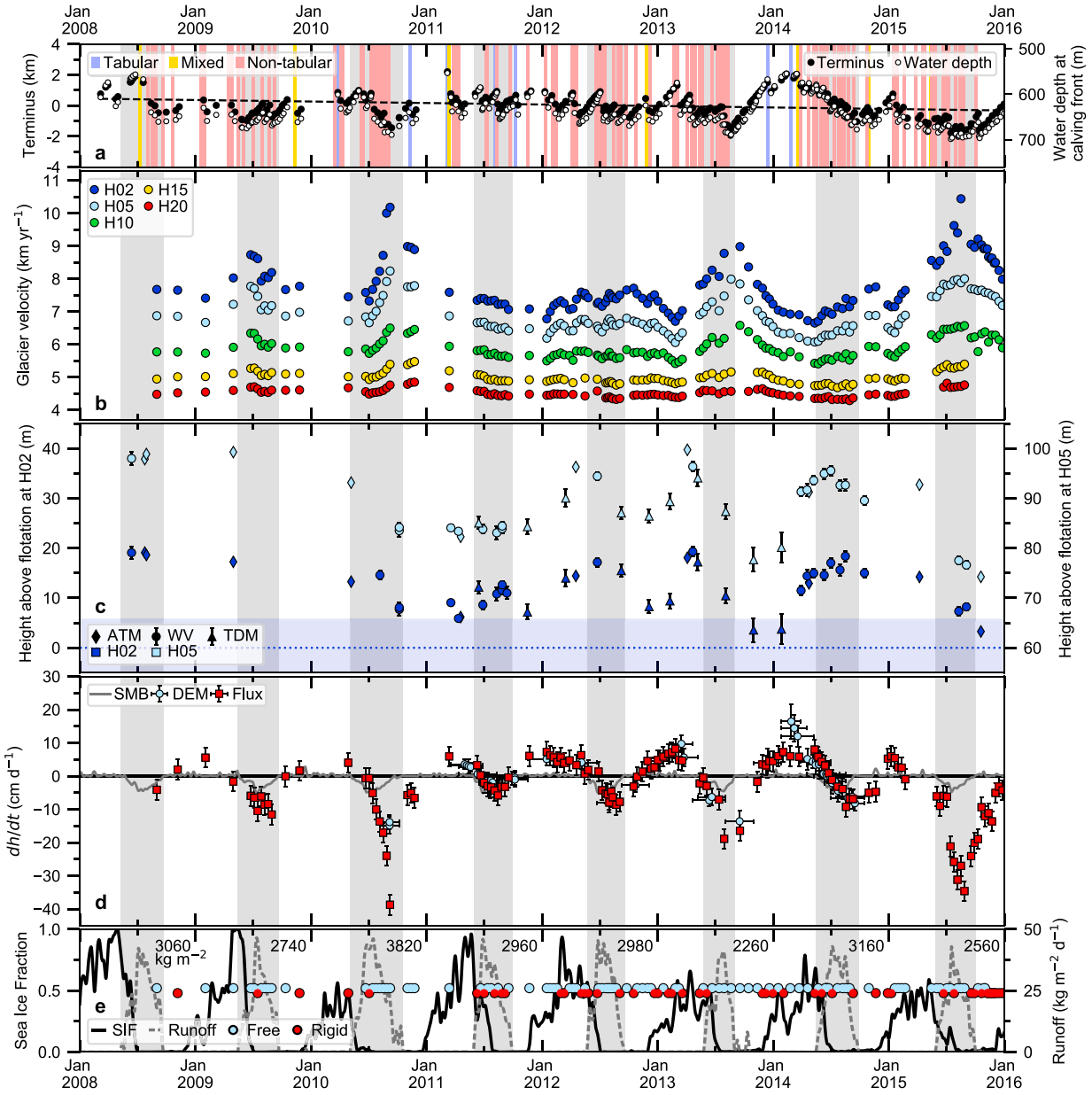

Figure 3. Observational record for Helheim. (a) Terminus position relative to the 2008–2016 average, water depth at the calving front, and calved iceberg type. (b) Glacier velocity at sample points H02–H20 in Figure 1a. (c) Height above flotation at H02 and H05. (d) Surface-elevation change rates from the DEM and fluxgate methods. (e) Ice-mélange conditions from TSX velocity estimates, sea ice fraction from OSTIA, and surface runoff from RACMO2.3. The dashed line in Figure 3a shows the linear trend in the observed terminus positions. The blue dotted line in Figure 3c indicates the height where H02 should become afloat with 50 m uncertainties in the bed elevation indicated by the shaded bar. The gray line in Figure 3d shows the surface-elevation change rate due to surface mass balance processes predicted by RACMO2.3. Text above runoff curve in Figure 3e indicates the total surface runoff for each year. The blue and red circles in Figure 3e indicate free and rigid ice-mélange conditions, respectively. The vertical shaded bars indicate periods of surface runoff.

2.7. Glacier Surface Runoff, Ice-Mélange Rigidity, and Sea Ice Fraction

While many different oceanic and atmospheric changes can affect tidewater glacier dynamics, in this study we focused primarily on the effects of surface melt and ice-mélange rigidity. To quantify surface melt, we used daily, modeled surface runoff from RACMO2.3. We sampled surface runoff at the same grid cells that we used for our surface-elevation change rate calculations (section 2.6). The magnitudes of the surface runoff estimates are sensitive to RACMO's spatial resolution [*Noël et al.*, 2016], so we primarily used these estimates to define the surface melt season.

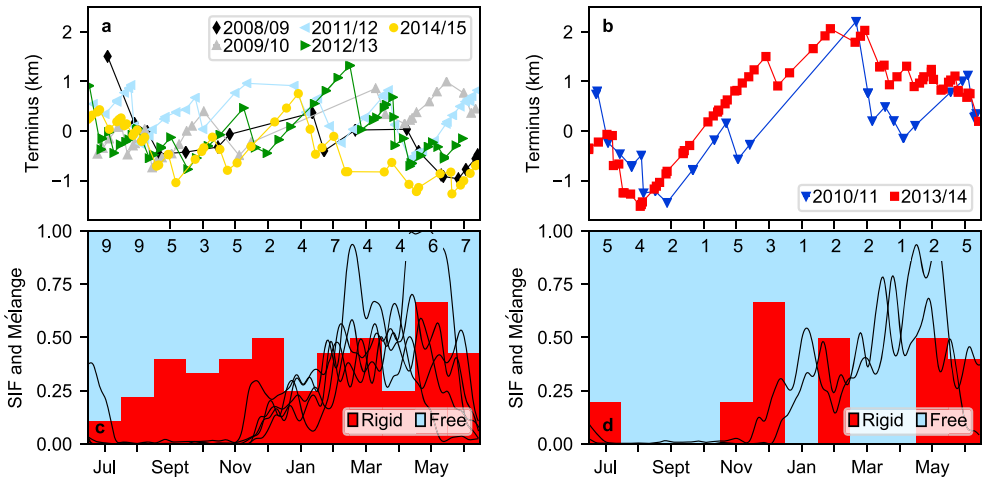

Figure 4. (a and b) Terminus position and (c and d) SIF and ice-mélange conditions during years when Helheim (right) did and (left) did not seasonally advance by >3 km. Ice-mélange conditions have been monthly binned for all years in each panel. The numbers indicate the total number of TSX velocity estimates used in each binning.

To assess ice-mélange rigidity, we used the TSX velocity estimates from speckle tracking. If speckle tracking can determine a velocity in the ice mélange, then the ice mélange is likely rigid or nearly rigid; if speckle tracking cannot determine a velocity, then the ice mélange is free to move around [*Joughin et al.*, 2008a]. We characterized the ice mélange as "rigid" or "free" based on these criteria. Since rigid mélange is often linked to sea ice formation [*Amundson et al.*, 2010], we also reported sea ice fraction (SIF) from the Operational Sea Surface Temperature and Sea Ice Analysis (OSTIA) system, which estimates daily SIF at 10 km resolution by combining in situ measurements with satellite data from the Group for High Resolution Sea Surface Temperature [*Donlon et al.*, 2012]. The SIF estimates have a threshold accuracy of ~20%. We sampled SIF at grid cells near the entrance to Sermilik (Helheim) and Kangerlussuaq Fjords.

3. Results

Using the methods outlined above, we produced a detailed record of terminus position, glacier velocity, surface elevation, and iceberg-calving behavior at Helheim and Kangerlussuaq from 2008 to 2016. Our observations indicate that Helheim and Kangerlussuaq behaved differently on a seasonal and interannal timescale.

3.1. Helheim Glacier

Figure 3 shows terminus position, iceberg-calving behavior, glacier velocity, surface elevation, surface-elevation change rate, ice-mélange rigidity, sea ice fraction, and surface runoff at Helheim from 2008 to 2016. Helheim's mean terminus position from 2008 to 2016 was 4.5 km upstream of its May 2001 position (Figure 1b). The glacier retreated by 100 ± 20 m/yr from 2008 to 2016 (p value of 10^{-6} from the linear regression), with seasonal variations in terminus position superimposed on this long-term trend. The glacier reached its position of maximum seasonal retreat in late summer during seven out of the eight years and its position of maximum advance in late winter during at least five of those years. Nontabular iceberg calving accounted for 105 (86%) of the 122 observed calving episodes at Helheim (Figure 3a). Glacier velocity varied seasonally during some years by up to 3 km yr^{-1}, with peak velocities occurring in late summer (Figure 3b). Surface elevations varied seasonally by ~10–20 m at H02 and H05 (Figure 3c), with glacier thickening rates peaking in January to March and glacier thinning rates peaking in August to September (Figure 3d).

The two largest seasonal changes in terminus position occurred in 2010/2011 and 2013/2014, when Helheim retreated and advanced over a range of >3 km. In 2010, Helheim retreated 2.3 km down a reverse bed slope from early July to mid-September. During the retreat, the glacier sped up by 1.6 km yr^{-1} (24%) at H05 and by 0.4 km yr^{-1} (8%) at H20, reaching a peak velocity in September at H05 and in late November at H20. Helheim

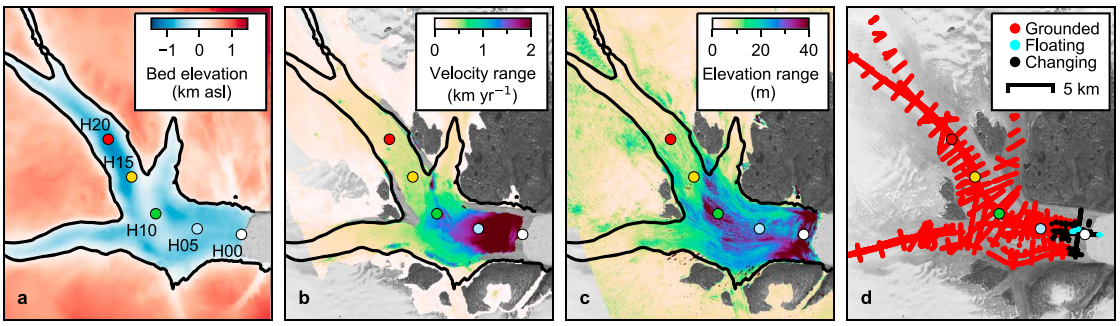

Figure 5. Range of observed glacier velocities and surface elevations at Helheim from 2011 to 2015. All linear trends have been removed before calculating the range. (a) Bed elevation from *Morlighem et al*. [2014], (b) range of observed glacier velocities, (c) range of observed surface elevations, and (d) the resulting changes in the flotation condition. Regions in red remained grounded, regions in blue remained floating, and regions in black changed between grounded and floating. The black curve in Figures 5a–5c indicates the region where the bed is below sea level.

then slowed as its terminus readvanced 3.5 km to the crest of the reverse bed slope by mid-March 2011 (Figure 1c). Similarly, in 2013, Helheim retreated 2.8 km down the reverse bed slope from early March to mid-August, with a subsequent readvance of 3.6 km to the top of the reverse bed slope by mid-February 2014. During this 2013 retreat, the glacier sped up by 1.9 km yr^{-1} (32%) at H05 and by 0.3 km yr^{-1} (6%) at H20, again reaching a maximum velocity in September at H05 and in late November at H20. Helheim also thinned by ~20 m at H02 and H05 during this retreat. At H02, the glacier thinned to flotation and a floating ice tongue formed downstream (Movie S1 in the supporting information). Although the available surface-elevation measurements do not cover winter 2010/2011, surface elevations collected before and after the winter indicate that Helheim may have thinned to flotation at H02 during the 2010 retreat as well. Furthermore, glacier thinning rates exceeded 15 cm d^{-1} during summers 2010, 2013, and 2015 but were closer to 5 to 10 cm d^{-1} during summers 2011, 2012, and 2014. Modeled thinning rates from surface mass balance processes were <5 cm d^{-1} during all summers, indicating that the observed thinning occurred primarily due to a change in ice dynamics [*Bevan et al*., 2015]. Helheim calved nontabular icebergs during the 2010 and 2013 seasonal retreats. The seasonal advances ended when the terminus reached the top of the reverse bed slope from where it calved several large tabular icebergs. The ice mélange was generally less rigid during years when large seasonal retreats and advances occurred, as shown in Figure 4.

Figure 5 shows the range of observed glacier velocities and surface elevations at Helheim from 2011 to 2015. We removed all linear trends before calculating the range for each grid cell. The largest variations in glacier velocity and surface elevation occurred within ~10 km of the calving front. Figure 5d shows how the surface-elevation variations affected the flotation condition at each CReSIS bed-elevation measurement (section 2.5). For a large region downstream of H05, the glacier changed between floating and grounded from 2011 to 2015. For regions upstream of H05, the glacier remained grounded. When the glacier advanced to the top of the reverse bed slope at +2 km (Figure 1c), its terminus was always floating.

3.2. Kangerlussuaq Glacier

Figure 6 shows terminus position, iceberg-calving behavior, glacier velocity, surface elevation, surface-elevation change rate, ice-mélange rigidity, sea ice fraction, and surface runoff at Kangerlussuaq from 2008 to 2016. Kangerlussuaq's mean terminus position from 2008 to 2016 was 4.0 km upstream of its May 2001 position (Figure 2b). The glacier advanced by 200 ± 30 m yr^{-1} from 2008 to 2016 (p value of 10^{-8} from the linear regression), with seasonal variations in terminus position of >3 km superimposed on this long-term trend during six out of the eight years. The two years without a pronounced seasonal cycle in terminus position were 2010 and 2011.

Typically, Kangerlussuaq advanced from December to late June or mid-July and then retreated until December (Figure 6a). Few icebergs calved during the seasonal advance. The late-summer retreat started with the calving of large tabular icebergs, which transitioned to mixed and nontabular icebergs as the

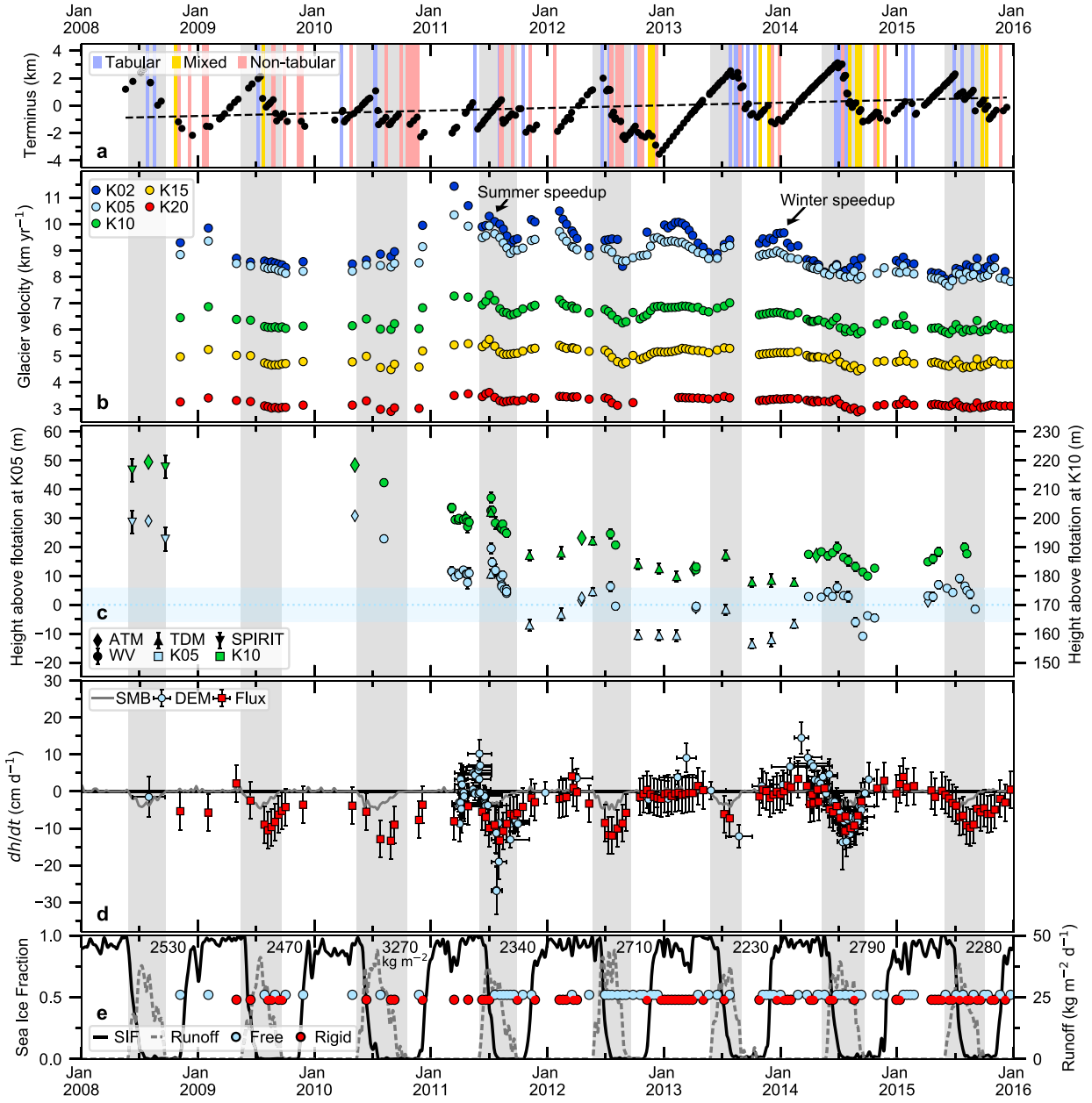

Figure 6. (a–e) Observational record for Kangerlussuaq. Subpanels are the same as in Figure 3. Note that Figure 6c shows height above flotation at K05 and K10. The light blue dotted line in Figure 6c indicates the height where K05 should become afloat with 50 m uncertainties in the bed elevation indicated by the shaded bar.

retreat continued. Nontabular iceberg calving accounted for 36 (47%) of the 77 observed calving episodes at Kangerlussuaq. Figure 7 compares the timing of seasonal changes in terminus position to changes in ice-mélange rigidity and sea ice fraction. The timing of the seasonal transition from retreat to advance corresponded well with the seasonal transition to more rigid mélange and denser sea ice conditions.

Kangerlussuaq's velocity varied on both seasonal and interannual timescales (Figure 6b). Glacier velocity typically increased from late summer to midwinter and then decreased again until late summer at all sample points. This "winter speedup" was most pronounced during winter 2010/2011, when the glacier sped up by 2.1 km yr^{-1} (25%) at K05 and by 0.5 km yr^{-1} (16%) at K20. The winter speedup then decreased in magnitude from 2011 to 2015. The glacier also slowed over this time period, with glacier velocity decreasing by 400 m yr^{-2} at K05 and by 70 m yr^{-2} at K20, as shown in Figure 8a. By 2015, Kangerlussuaq's velocity was

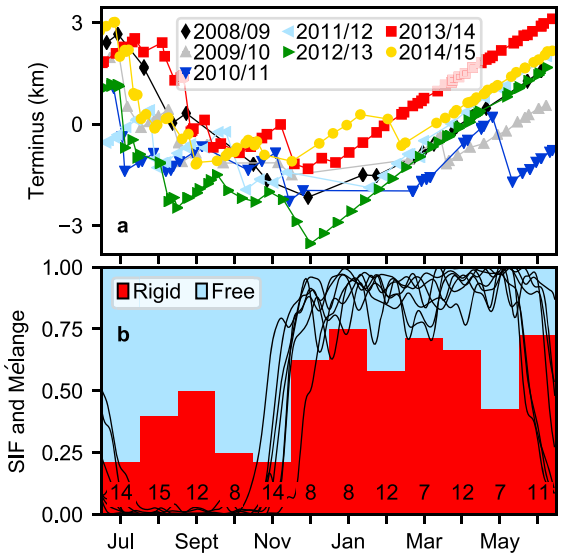

Figure 7. (a) Terminus position and (b) SIF and ice-mélange conditions at Kangerlussuaq. Ice-mélange conditions have been monthly binned, with the number indicating the total number of TSX velocity estimates used in each binning.

similar to its velocity before the 2010/2011 winter speedup event. Kangerlussuaq also sped up by ~200–400 m yr^{-1} (~5–10%) at all sample points during the mid summer.

Kangerlussuaq continued to thin through 2015, with thinning rates generally decreasing from 2001 to 2015 (Figures 2b and 6c) [*Howat et al.*, 2011]. By late summer 2011, the glacier had thinned to flotation at K05 (Movie S2), with surface elevations remaining at or below the flotation threshold through 2015. The greatest thinning rates (6 ± 1 to 12 ± 1 m yr^{-1}) from 2011 to 2015 occurred near K20, as shown in Figure 8b. Seasonal variations in surface elevation of ~20 m at K05 and ~10 m at K10 were superimposed on the long-term thinning. Seasonal thinning generally started in May or June, reached a maximum rate of 10–15 cm d^{-1} in July or August, and ended by September to November (Figure 6d). Glacier thickening typically peaked in March. Thinning rates from surface mass balance processes were <5 cm d^{-1} during all summers, indicating that the observed thinning occurred primarily due to a change in ice dynamics.

Figure 9 shows the range of observed glacier velocities and surface elevations at Kangerlussuaq from 2011 to 2015. All linear trends (Figure 8) were removed before calculating the range for each grid cell. The largest variations in glacier velocity and surface elevation occurred near the terminus. Figure 9d shows how the surface-elevation variations affected the flotation condition at each CReSIS bed-elevation measurement. (Note that while we removed many of the bed-elevation measurements that were collected over Kangerlussuaq's floating ice tongue, that the remaining measurements might still have large uncertainties.)

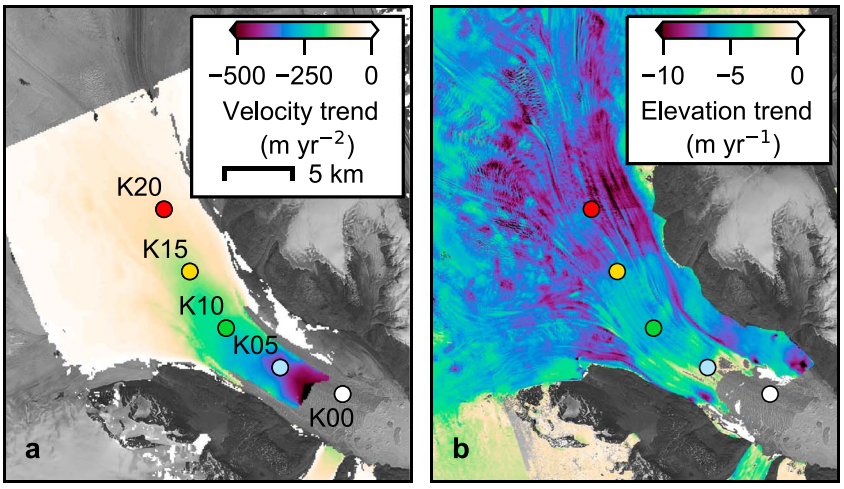

Figure 8. Linear trends in (a) glacier velocity and (b) surface elevation (i.e., average thinning rate) from 2011 to 2015 at Kangerlussuaq. All plotted trends have a p value < 0.05.

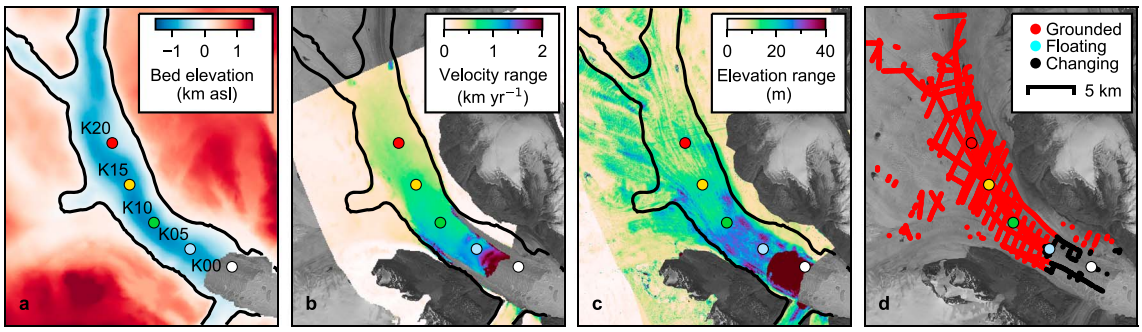

Figure 9. (a–d) Range of observed glacier velocities and surface elevations from 2011 to 2015 at Kangerlussuaq. See Figure 5 for a description of the subpanels.

The region downstream of K05 changed between grounded and floating from 2011 to 2015, while the region upstream of K05 remained grounded.

4. Discussion

Despite extensive dynamic mass loss from many Greenland tidewater glaciers over the last two decades, there has also been significant spatiotemporal variability in the dynamic response of individual glaciers [*Moon and Joughin*, 2008; *Moon et al*., 2012; *Enderlin et al*., 2014]. Regional climatic and oceanographic differences likely account for some of this variability [*Inall et al*., 2014; *Jensen et al*., 2016]. In addition, individual glacier characteristics, such as glacier geometry, have also likely contributed [*Enderlin et al*., 2013; *Felikson et al*., 2017]. In the next sections, we discuss the interplay between glacier geometry and environmental change in determining the multiyear evolution, seasonal dynamics, and terminus behavior of Helheim and Kangerlussuaq Glaciers from 2008 to 2016.

4.1. Long-Term Behavior From 2008 to 2016

Many Greenland tidewater glaciers, including Helheim and Kangerlussuaq, rapidly retreated and accelerated during a period of above-average oceanic and atmospheric temperatures in the early 2000s [*Joughin et al*., 2004; *Rignot et al*., 2004; *Howat et al*., 2007, 2008; *Hanna et al*., 2009; *Murray et al*., 2010]. While some glaciers, such as Greenland's largest glacier, Jakobshavn Isbrae, have continued to retreat and thin [*Joughin et al*., 2004, 2012], other glaciers have returned to more stable terminus positions. Helheim and Kangerlussuaq ended their terminus retreats by 2006 [*Joughin et al*., 2008b; *Bevan et al*., 2012], but Helheim stopped thinning shortly thereafter (Figure 3c) [*Howat et al*., 2011], while Kangerlussuaq continued thinning through 2015 (Figure 6c). Helheim's terminus likely remained stable from 2008 to 2016 due to shallower water depths only a few kilometers farther upstream (Figure 1c), which may have limited its retreat over the last century [*Joughin et al*., 2008b; *Andresen et al*., 2012]. Based on the available bed-elevation measurements, no such shallower water depths or lateral constrictions in glacier width likely existed near Kangerlussuaq's grounding line to prevent further grounding-line retreat from 2008 to 2016 (Figure 2c). While there may be shallower water depths farther down fjord, if this is the case, the glacier does not appear to be reaching them. Instead, Kangerlussuaq's multiyear evolution from 2008 to 2016 appears to have been governed primarily by grounding-line retreat through a basal overdeepening.

As Kangerlussuaq thinned following its 2004/2005 retreat [*Howat et al*., 2011], its terminus changed from grounded to floating. By winter 2011/2012, the glacier had a roughly 5 km long floating ice tongue (Figure 2c), which may have increased the glacier's susceptibility to submarine melt [*Motyka et al*., 2011; *Truffer and Motyka*, 2016]. During late winter 2010 through late summer 2011, a section of this floating ice tongue likely ungrounded (K05 in Figure 6c), primarily over an area with unknown bed geometry (Figure 2c and Movie S2). We suggest that there is a basal overdeepening in this region (red circle in Figure 2c), because surface-elevation measurements collected when the glacier was still grounded in this region from 2001 to 2008 indicate a flat or reverse surface slope (Figure 2b) [*Budd*, 1970]. Consequently, grounding-line retreat into this overdeepening caused speedup and thinning (Figure 6). This thinning diffused inland through a steepening of surface slopes (Figure S4) [*Howat et al*., 2007], and by 2015 the pattern of strongest thinning was centered ~20 km inland from the calving front (K20 in Figure 8b). While this

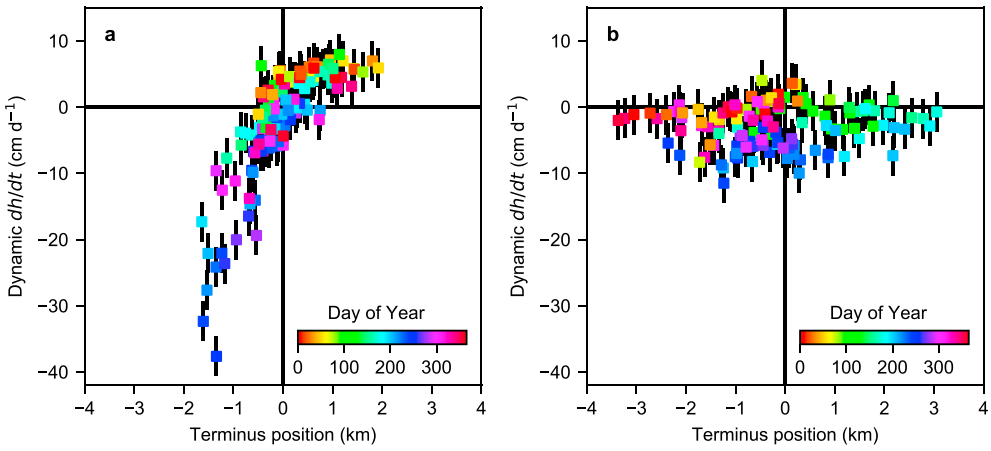

Figure 10. Relationship between the terminus position and dynamic surface-elevation change rate (first term on the right in equation (1)) at (a) Helheim and (b) Kangerlussuaq. Terminus position is relative to the mean 2008–2016 terminus position. The marker color indicates the day of year.

ungrounding event occurred during a period of above-average sea surface temperatures near the entrance to Kangerlussuaq Fjord [*Inall et al.*, 2014], it likely would have occurred even in the absence of this warming due to dynamic feedbacks associated with grounding-line retreat into deeper water [*Schoof*, 2007]. By winter 2011/2012, Kangerlussuaq's grounding line had retreated into shallower water. Kangerlussuaq has since slowed and reduced its dynamic thinning rates (Figures 8a and 6c), potentially signaling that its grounding line is in a more stable position now that it rests on a down-glacier bed slope [*Schoof*, 2007] in a region where the fjord narrows (K05 in Figure 2a) [*Enderlin et al.*, 2013].

4.2. Seasonal Variations in Glacier Velocity and Surface Elevation

Seasonal variations in glacier velocity are often linked to seasonal changes in terminus position or surface-melt-induced basal lubrication [*Howat et al.*, 2010; *Moon et al.*, 2014]. While less is known about seasonal dynamic thinning and thickening, they have also been connected to these processes [*Joughin et al.*, 2012; *Bevan et al.*, 2015]. For a lightly grounded glacier retreating into deeper water, terminus position serves as a proxy for water depth at the grounding line (e.g., Figure 3a), and consequently, terminus position affects glacier velocity by modulating the force balance at the terminus [*Cuffey and Paterson*, 2010]. However, if a glacier has a large floating section, this relationship may not hold, particularly if there is little side drag where the floating section comes in contact with the fjord walls. At Jakobshavn, for example, glacier velocity and terminus position were highly correlated when the terminus was grounded but not when the terminus was floating [*Joughin et al.*, 2012]. Terminus variations can cause large seasonal speedups of $>$30% [*Moon et al.*, 2014], while surface-melt-induced basal lubrication has been shown to cause more modest speedups of $<$10–15% [*Joughin et al.*, 2008c; *Moon et al.*, 2014].

Our results show that changes in terminus position and related dynamic feedbacks likely caused the observed seasonal variations in glacier velocity and surface elevation at Helheim (Figure 3). This hypothesis is contrary to the conclusions of *Bevan et al.* [2015], who suggested that seasonal dynamic thinning resulted from surface-melt-induced basal lubrication at Helheim. Despite evidence that surface melt drains to the bed at Helheim [*Everett et al.*, 2016; *Poinar et al.*, 2017], surface-melt-induced basal lubrication has been shown to cause only small speedups of $<$5% on this glacier [*Andersen et al.*, 2010]. Iceberg-calving events, on the other hand, have been shown to coincide with much larger speedups at timescales of minutes to weeks [*Howat et al.*, 2005; *Nettles et al.*, 2008; *Murray et al.*, 2015]. Consistent with prior results, we observed the greatest seasonal speedups and dynamic thinning when Helheim's terminus was most retreated during the summers of 2010 and 2013 (Figure 3). This relationship is clearly illustrated in Figure 10a, which plots the dynamic surface-elevation change rate (first term in equation (1)) against the terminus position. When Helheim's terminus position was down fjord (up fjord) of its mean terminus position from 2008 to 2016, the glacier dynamically thickened (thinned), suggesting that the mean 2008–2016 terminus position

closely corresponded with the location where the ice flux was equal to the balance flux. Consequently, Helheim's dynamic surface-elevation change rate primarily depended on the terminus position along the reverse bed slope, not on whether the glacier was presently advancing or retreating. These results confirm the findings of other studies, which have shown that Helheim is highly sensitive to changes at the terminus [*Howat et al*., 2005; *Nick et al*., 2009].

By contrast, seasonal variations in glacier velocity and surface elevation appeared to be more complex at Kangerlussuaq. We observed two distinct periods of seasonal speedup at Kangerlussuaq: one in the summer and one in the winter (Figure 6b). The summer speedup of 5–10% occurred around the time of peak surface melt. During summers 2011 and 2013, this speedup occurred while the terminus was still advancing, indicating that the speedup was not related to terminus retreat. Instead, surface-melt-induced basal lubrication likely caused this speedup [*Sundal et al*., 2013], which was similar in magnitude to the magnitude of surface-melt-induced speedups observed at Helheim [*Andersen et al*., 2010] and at other glaciers [*Moon et al*., 2014]. Furthermore, all sample points showed an abrupt, synchronous velocity increase during this speedup, which may imply widespread basal lubrication across the lower glacier. The winter speedup, on the other hand, occurred when the terminus was most retreated, suggesting that the speedup resulted from reduced ice-shelf buttressing driven by terminus retreat.

In comparison to our findings at Helheim, there is no clear relationship between terminus position and the dynamic surface-elevation change rate at Kangerlussuaq (Figure 10b). Based on the similarity in timing between the summer speedup and seasonal dynamic thinning (Figure 6), it is possible that surface-melt-induced basal lubrication caused some dynamic thinning at Kangerlussuaq. However, even during summers with very small speedup events, such as summer 2009, we observed dynamic thinning of a similar magnitude to that observed during other summers (Figure 6). Consequently, other processes likely contributed to the observed dynamic thinning at Kangerlussuaq. While both changes in the ice-thickness and velocity gradients can affect the surface-elevation change rate (equation (1)), our results indicate that an increase in the velocity gradient typically accounted for ~75% of the observed seasonal dynamic thinning at Kangerlussuaq (~6 cm d^{-1} of ~8 cm d^{-1}; Text S2). Changes in the velocity gradient could have resulted from several different processes, including thinning-induced changes in the effective pressure [*Howat et al*., 2005] and changes in the terminus or grounding-line position [*Nick et al*., 2009]. However, inopportune gaps in our record make it difficult to determine which of these processes contributed to seasonal dynamic thinning at Kangerlussuaq.

The different dynamic responses of Helheim and Kangerlussuaq to seasonal changes in terminus position are not surprising given differences in the spatial extent of floating ice near their termini (Figure 10). For a lightly grounded glacier, such as Helheim, terminus retreat into deeper water reduces basal and lateral resistance to flow and increases the ice thickness at the grounding line. Both of these processes require the glacier to speed up to restore force balance [*Howat et al*., 2005]. For a glacier with a floating terminus confined within a narrow fjord, such as Kangerlussuaq, terminus retreat only reduces lateral resistance to flow, and consequently, a smaller speedup is likely necessary to restore force balance. As a result, despite larger seasonal terminus variations at Kangerlussuaq than at Helheim, glacier velocities and surface elevations were more sensitive to terminus position at Helheim than at Kangerlussuaq (Figures 3 and 6).

At both Helheim and Kangerlussuaq, variations in glacier velocity associated with seasonal terminus retreat and advance extended more than 25 km inland (Figures 5 and 9). Velocity variations likely extended this far inland through some combination of diffusion due to a steepening of surface slopes [*Howat et al*., 2005] and the initial perturbation in the force balance near the terminus [*Joughin et al*., 2012]. In regions where we observed the greatest seasonal velocity variability, recent modeling studies indicate a weak bed ($<$40 kPa) [*Shapero et al*., 2016], which should allow speedups associated with the initial perturbation in the force balance to extend farther inland [*Joughin et al*., 2012]. While seasonal speedups associated with the initial perturbation in the force balance should be synchronous across the lower glacier, diffusion should cause a lag between speedup near the terminus and speedup farther inland. During summers 2010 and 2013, Helheim started speeding up at all sample points around the same time, indicating that this initial speedup likely resulted from terminus retreat into deeper water (Figure 3b). Glacier velocity 20 km inland (H20), however, peaked several months after glacier velocity peaked near the terminus (H02). This secondary, delayed response diffused inland through a steepening of surface slopes (Figure S3). Consequently, both diffusion and bed strength likely contributed to the inland propagation of seasonal speedups at Helheim and Kangerlussuaq.

4.3. Seasonal Variability in Terminus Position and Iceberg-Calving Behavior

Seasonal variations in terminus position have been observed at many Greenland tidewater glaciers [*Howat et al*., 2010; *Seale et al*., 2011; *Schild and Hamilton*, 2013]. Typically, these variations are linked to oceanic or atmospheric changes that seasonally alter the iceberg-calving rate, such as changes in ice-mélange strength [*Amundson et al*., 2010], submarine melt [*O'Leary and Christoffersen*, 2013], and the availability of surface melt for hydrofracture [*Benn et al*., 2007]. While some tidewater glaciers show a clear relationship between seasonal terminus variations and oceanic and atmospheric changes, other glaciers indicate a more complex relationship [*Schild and Hamilton*, 2013]. At Helheim, for example, *Schild and Hamilton* [2013] observed seasonal retreats that varied in magnitude by 2 km/yr and in timing of onset by 60 days. We also observed significant variability in seasonal terminus variations at Helheim (Figure 3a). Our results suggest that this variability was partially related to seasonal dynamic thinning and thickening, which altered the spatial extent of floating ice near the terminus (Figure 3c). Furthermore, seasonal terminus variations were likely larger at Kangerlussuaq than at Helheim due to the presence of its year-round floating ice tongue.

When Helheim and Kangerlussuaq formed floating ice tongues, iceberg calving ceased during the winter and both glaciers seasonally advanced by >3 km. These large seasonal advances occurred every winter at Kangerlussuaq but only during winters 2010/2011 and 2013/2014 at Helheim (Figures 3a and 6a). At Kangerlussuaq, seasonal advances occurred when more rigid ice mélange formed in the fjord (Figure 7), which likely suppressed iceberg calving [*Amundson et al*., 2010; *Seale et al*., 2011]. At Helheim, however, the ice mélange appeared to be similarly strong, if not slightly weaker, during winters when a floating ice tongue formed (Figure 4), likely indicating that large seasonal advances at Helheim did not result from changes in ice-mélange strength. Large seasonal retreats at Helheim, however, did occur during weaker mélange conditions (Figures 3e and 4), suggesting that the ice mélange may still have affected iceberg-calving rates during other seasons. This result contradicts the conclusions of *Cook et al*. [2014], who used a numerical model to show that changes in ice-mélange strength had little effect on Helheim's terminus position. While it is possible that another oceanic or atmospheric change, such as changes in submarine melt [*Straneo et al*., 2011], can explain the varying magnitude of seasonal advances at Helheim, we suggest that these large seasonal advances followed summers with substantial dynamic thinning for a reason: this thinning caused the terminus to evolve from grounded to floating (Figure 3c and Movie S1), which affected iceberg-calving rates.

Iceberg calving is sensitive to the spatial extent of floating ice near the terminus [*Benn et al*., 2007]. At the two extremes, grounded tidewater glaciers in Alaska and Greenland calve frequent, small nontabular icebergs, and floating ice shelves in Antarctica calve infrequent, large tabular icebergs [*Walter et al*., 2010; *Bassis and Jacobs*, 2013]. Similarly, Helheim and Kangerlussuaq typically calved nontabular icebergs when their termini were grounded or nearly grounded and tabular icebergs when their termini were floating (Figures 3 and 6) [*Joughin et al*., 2008b]. Helheim calved nontabular icebergs year-round but rarely calved tabular icebergs during the winter, which may indicate that different processes affect nontabular and tabular iceberg calving [*Benn et al*., 2007; *Amundson et al*., 2010]. For example, near-terminus deviatoric stresses and strain rates tend to be smaller for a floating rather than grounded terminus, which likely causes slower rates of rift propagation and thereby promotes tabular iceberg calving [*Reeh*, 1968; *Alley et al*., 2008]. When tabular icebergs do calve from the terminus, these icebergs typically remain upright; nontabular icebergs, on the other hand, will likely overturn, which may promote further iceberg calving by flushing the ice mélange further away from the terminus [*Amundson et al*., 2010]. Consequently, even if oceanic and atmospheric conditions were similar during different winters at Helheim, the glacier may only have been able to readvance by >3 km following summers with significant dynamic thinning, which affected iceberg-calving behavior.

Our results also suggest that nontabular iceberg calving at Helheim occurred as a lightly grounded terminus is forced up a reverse bed slope [*Joughin et al*., 2008b], contrary to the hypothesis of *James et al*. [2014]. If that is the case, then seasonal dynamic thinning may lessen this geometric effect, further enabling the terminus to readvance. As has been observed in other studies [*Joughin et al*., 2008b; *James et al*., 2014; *Murray et al*., 2015], large rifts and depressions often formed within ~500 m of the calving front before nontabular iceberg calving at Helheim (Movie S1). We did not observe any such rifts or depressions in the DEMs or satellite images before nontabular iceberg calving at Kangerlussuaq (Movie S2). It is possible that rifts formed at Kangerlussuaq, but we did not observe them. However, this lack of observations may also imply that nontabular iceberg calving occurred through a different mechanism there, perhaps because Kangerlussuaq typically had a floating, rather than lightly grounded, terminus.

The rifts and depressions that form before nontabular iceberg calving at Helheim have been interpreted in two different ways. *Joughin et al*. [2008b] suggested that these depressions form as the terminus is pushed up a reverse bed slope faster than it can thin to flotation, while a region upstream remains at or near flotation. Deviatoric stresses in this depression should be sensitive to the basal topography and to the ice thickness near the terminus, since thicker ice will need to be forced farther up this reverse bed slope. Once a rift forms in this depression, enhanced rift growth may occur due to the strain-rate -weakening nature of ice [*Bassis and Ma*, 2015]. By contrast, *James et al*. [2014] interpreted these depressions as "flexion zones," which form as the calving front advances into deeper water faster than it can viscously adjust to the buoyant disequilibrium. The ice must then adjust by brittle failure, causing the calving front to rotate outward as a basal crevasse penetrates at depth. Based on the available bed-elevation measurements, Helheim's terminus advanced into shallower water during nontabular iceberg calving (Figure 1c). *James et al*. [2014] suggested that these bed-elevation measurements might be unreliable, but the bed-elevation measurements have since been reprocessed, and we used those measurements in this study. Furthermore, Helheim's high sensitivity to terminus position also implies retreat down a reverse bed slope (Figure 10a) [*Nick et al*., 2009]. If rates of dynamic thinning and submarine melt were greater than the rate at which the calving front advanced into shallower water, then the calving front may still have come ungrounded [*James et al*., 2014; *Murray et al*., 2015]. However, when Helheim advanced to the top of the reverse bed slope and calved into deeper water, the terminus typically calved tabular rather than nontabular icebergs. These observations may indicate that rift-driven, nontabular iceberg calving typically occurs when a lightly grounded terminus is resting on a reverse bed slope. Consequently, seasonal dynamic thinning and thickening may affect nontabular iceberg-calving rates by altering deviatoric stresses in the depression that forms upstream of the calving front.

While a full analysis of this mechanism and other potential controls on nontabular and tabular iceberg calving is outside the scope of this study, our results highlight that seasonal terminus variations are affected by the spatial extent of floating ice near the terminus. For a lightly grounded glacier, such as Helheim, seasonal dynamic thinning and thickening can affect this spatial extent, which in turn affects iceberg calving. Consequently, temporal changes in the extent of floating ice may help explain why some glaciers, such as Helheim, show a clear seasonal pattern in terminus position and glacier velocity during some years but not during other years [*Howat et al*., 2010; *Schild and Hamilton*, 2013; *Moon et al*., 2014].

5. Conclusions

Our observations indicate that glacier geometry exerted a strong control on the seasonal and interannual evolution of Helheim and Kangerlussuaq from 2008 to 2016. These results are consistent with prior studies at Helheim and Kangerlusssuaq [*Howat et al*., 2007; *Nick et al*., 2009] and at other glaciers [e.g., *Joughin et al*., 2012; *Motyka et al*., 2017]. While Helheim stopped thinning shortly after its 2001–2005 retreat ended, Kangerlussuaq continued thinning through 2015. This thinning initially caused grounding-line retreat into deeper water, likely leading to further speedup, thinning, and retreat. By late summer 2011, Kangerlussuaq's grounding line had retreated into shallower water. Kangerlussuaq has since slowed and reduced its dynamic thinning rates, suggesting that its grounding line may be in a more stable position now that it rests on a down-glacier bed slope. Helheim's stable grounding-line position from 2008 to 2016 appears to be related to a down-glacier bed slope a few kilometers upstream of its terminus position. Given that both Helheim and Kangerlussuaq flow through basal troughs that become narrower and shallower $<$20 km upstream of their current grounding-line positions, the potential retreat of these glaciers over the next few centuries appears to be limited [*Nick et al*., 2013].

We also observed different seasonal variability in terminus position, glacier velocity, surface elevation, and iceberg-calving behavior at Helheim and Kangerlussuaq, which we partially attribute to differences in ice dynamics related to the glaciers' geometries. Despite larger seasonal retreats at Kangerlussuaq than at Helheim, glacier velocity and surface elevation were more sensitive to terminus position at Helheim than at Kangerlussuaq. Helheim is likely more sensitive to terminus position due to its lightly grounded, rather than floating, terminus. Iceberg-calving behavior also depended on glacier geometry, with tabular iceberg calving typically indicating a floating terminus and rift-driven, nontabular iceberg calving indicating a lightly grounded terminus resting on a reverse bed slope. Our results suggest that seasonal velocity variability and

iceberg-calving behavior may provide additional clues about glacier geometry where we presently have limited bed- and surface-elevation measurements.

Given that seasonal elevation variations alter glacier geometry, these elevation variations may also affect the dynamic response of tidewater glaciers to environmental change. Many studies [*Schild and Hamilton*, 2013; *Moon et al*., 2014] have found a clear, seasonal relationship between terminus position and environmental change at some tidewater glaciers, while other glaciers indicate a more complex relationship. Our results suggest that lightly grounded glaciers may be more likely to exhibit an inconsistent relationship between terminus position and environmental change, because seasonal elevation variations can affect the spatial extent of floating ice near their termini and thereby influence iceberg-calving behavior. Consequently, the effect of an oceanic or atmospheric change on tidewater glacier dynamics may differ depending on when the change occurs relative to seasonal changes in glacier geometry. Long-term observations of seasonal elevation change are currently only available for a few tidewater glaciers in Greenland; however, seasonal dynamic thinning/thickening is likely widespread, and further research is needed to better understand its importance for the long-term evolution of the Greenland Ice Sheet.

Acknowledgments
L.M. Kehrl was supported by the Department of Defense (DoD) through the National Defense Science and Engineering Graduate Fellowship (NDSEG) Program, I. Joughin was supported by the NSF Office of Polar Programs (NSF-OPP) through the Center for Remote Sensing of Ice Sheets (CReSIS) (NSF ANT-0424589), D.E. Shean was supported by a NASA NESSF fellowship (NNX12AN36H), and L. Krieger was supported by Deutsche Forschungsgemeinschaft (DFG, FL 848/1-1). The TerraSAR-X and TanDEM-X data were provided by the German Aerospace Center (DLR), projects HYD0754 and XTI_GLAC0400. NASA's MEaSUREs Program (NNX08AL98A and NNX13AI21A) supported the SAR processing. Velocity data are available from the National Snow and Ice Data Center (nsidc.org/data/measures/gimp). We acknowledge bed-elevation measurements from CReSIS (ANT-0424589 and NNX10AT68G) and surface-elevation measurements from NASA's Airborne Topographic Mapper (ATM) Program. We thank Claire Porter, Paul Morin, and others at the Polar Geospatial Center (NSF ANT-1043681), who managed tasking, ordering, and distribution of the WorldView/GeoEye stereo-imagery. Resources supporting the Worldview DEM processing were provided by the NASA High-End Computing (HEC) Program through the NASA Advanced Supercomputing (NAS) Division at Ames Research Center. SPOT-5 DEMs and imagery were provided at no cost by the French Space Agency (CNES) through the SPIRIT International Polar Year project. RACMO2.3 data were kindly provided by Brice Noël and Michiel van den Broeke (Utrecht University). This study used sea ice fraction from the Operational Sea Surface Temperature and Sea Ice Analysis System (OSTIA) from the Copernicus Marine Service. Other data are available from the author upon request. We thank Editor Bryn Hubbard and two anonymous reviewers for their helpful comments that improved the quality and clarity of this manuscript.

References

Alley, R. B., H. J. Horgan, I. R. Joughin, K. M. Cuffey, T. K. Dupont, B. R. Parizek, S. Anandakrishan, and J. Bassis (2008), A simple law for ice-shelf calving, *Science*, *322*, 1344.

Amundson, J. M. (2016), A mass-flux perspective of the tidewater glacier cycle, *J. Glaciol.*, *62*(231), 82–93, doi:10.1017/jog.2016.14.

Amundson, J. M., M. A. Fahnestock, M. Truffer, J. Brown, M. P. Lüthi, and R. J. Motyka (2010), Ice mélange dynamics and implications for terminus stability, Jakobshavn Isbræ, Greenland, *J. Geophys. Res.*, *115*, F01005, doi:10.1029/2009JF001405.

Andersen, M. L., et al. (2010), Spatial and temporal melt variability at Helheim Glacier, East Greenland, and its effect on ice dynamics, *J. Geophys. Res.*, *115*, F04041, doi:10.1029/2010JF001760.

Andresen, C. S., et al. (2012), Rapid response of Helheim Glacier in Greenland to climate variability over the past century, *Nat. Geosci.*, *5*(1), 37–41, doi:10.1038/ngeo1349.

Bamber, J. L., et al. (2013), A new bed elevation dataset for Greenland, *Cryosphere*, *7*, 499–510, doi:10.5194/tc-7-499-2013.

Bassis, J. N., and S. Jacobs (2013), Diverse calving patterns linked to glacier geometry, *Nat. Geosci.*, *6*(10), 833–836, doi:10.1038/ngeo1887.

Bassis, J. N., and Y. Ma (2015), Evolution of basal crevasses links ice shelf stability to ocean forcing, *Earth Planet. Sci. Lett.*, *409*, 203–211, doi:10.1016/j.epsl.2014.11.003.

Benn, D. I., C. R. Warren, and R. H. Mottram (2007), Calving processes and the dynamics of calving glaciers, *Earth Sci. Rev.*, *82*, 143–179.

Bevan, S. L., A. J. Luckman, and T. Murray (2012), Glacier dynamics over the last quarter of a century at Helheim, Kangerdlugssuaq, and 14 other major Greenland outlet glaciers, *Cryosphere*, *6*(5), 923–937, doi:10.5194/tc-6-923-2012.

Bevan, S. L., A. J. Luckman, S. A. Khan, and T. Murray (2015), Seasonal dynamic thinning at Helheim Glacier, *Earth Planet. Sci. Lett.*, *415*, 47–53, doi:10.1016/j.epsl.2015.01.031.

Blair, B., and M. Hofton (2010), *IceBridge LVIS L2 Geolocated Ground Elevation and Return Energy Quartiles*, NASA Distributed Active Archive Centers, Natl. Snow and Ice Data Cent., Boulder, Colo.

Budd, W. F. (1970), Ice flow over bedrock perturbations, *J. Glaciol.*, *9*(55), 29–48.

Cook, S., I. C. Rutt, T. Murray, A. J. Luckman, T. Zwinger, N. Selmes, A. Goldsack, and T. D. James (2014), Modelling environmental influences on calving at Helheim Glacier in eastern Greenland, *Cryosphere*, *8*(3), 827–841, doi:10.5194/tc-8-827-2014.

Cuffey, K. M., and W. S. B. Paterson (2010), *The Physics of Glaciers*, 4th ed., Elsevier, Oxford.

Donlon, C. J., M. Martin, J. Stark, J. Roberts-Jones, E. Fiedler, and W. Wimmer (2012), The Operational Sea Surface Temperature and Sea Ice Analysis (OSTIA) system, *Remote Sens. Environ.*, *116*, 140–158, doi:10.1016/j.rse.2010.10.017.

Enderlin, E. M., I. M. Howat, and A. Vieli (2013), High sensitivity of tidewater outlet glacier dynamics to shape, *Cryosphere*, *7*, 1007–1015, doi:10.5194/tc-7-1007-2013.

Enderlin, E. M., I. M. Howat, S. Jeong, M. J. Noh, J. H. van Angelen, and M. R. Van Den Broeke (2014), An improved mass budget for the Greenland ice sheet, *Geophys. Res. Lett.*, *41*, 866–872, doi:10.1002/2013GL059010.

Everett, A., et al. (2016), Annual down-glacier drainage of lakes and water-filled crevasses at Helheim Glacier, southeast Greenland, *J. Geophys. Res. Earth Surf*, *121*, 1819–1833, doi:10.1002/2016JF003831.

Felikson, D., et al. (2017), Inland thinning on the Greenland ice sheet controlled by outlet glacier geometry, *Nat. Geosci.*, *10*(5), 366–369, doi:10.1038/ngeo2934.

Gudmundsson, G. H., J. Krug, G. Durand, L. Favier, and O. Gagliardini (2012), The stability of grounding lines on retrograde slopes, *Cryosphere*, *6*, 1497–1505, doi:10.5194/tc-6-1497-2012.

Hanna, E., J. Cappelen, X. Fettweis, P. Huybrechts, A. J. Luckman, and M. H. Ribergaard (2009), Hydrologic response of the Greenland ice sheet: The role of oceanographic warming, *Hydrol. Processes*, *23*, 7–30, doi:10.1002/hyp.7090.

Höhle, J., and M. Höhle (2009), Accuracy assessment of digital elevation models by means of robust statistical methods, *ISPRS J. Photogramm. Remote Sens.*, *64*(4), 398–406, doi:10.1016/j.isprsjprs.2009.02.003.

Holland, D. M., R. H. Thomas, B. De Young, M. H. Ribergaard, and B. Lyberth (2008), Acceleration of Jakobshavn Isbrae triggered by warm subsurface ocean waters, *Nat. Geosci.*, *1*, 659–664, doi:10.1038/ngeo316.

Howat, I. M., I. R. Joughin, S. Tulaczyk, and S. Gogineni (2005), Rapid retreat and acceleration of Helheim Glacier, east Greenland, *Geophys. Res. Lett.*, *32*, L22502, doi:10.1029/2005GL024737.

Howat, I. M., I. R. Joughin, and T. A. Scambos (2007), Rapid changes in ice discharge from Greenland outlet glaciers, *Science*, *315*(5818), 1559–1561, doi:10.1126/science.1138478.

Howat, I. M., I. R. Joughin, M. A. Fahnestock, B. E. Smith, and T. A. Scambos (2008), Synchronous retreat and acceleration of southeast greenland outlet glaciers 2000-06: Ice dynamics and coupling to climate, *J. Glaciol.*, *54*(187), 646–660.

Howat, I. M., J. E. Box, Y. Ahn, A. Herrington, and E. M. McFadden (2010), Seasonal variability in the dynamics of marine-terminating outlet glaciers in Greenland, *J. Glaciol.*, *56*(198), 601–613, doi:10.3189/002214310793146232.

Howat, I. M., Y. Ahn, I. R. Joughin, M. R. van den Broeke, J. T. M. Lenaerts, and B. E. Smith (2011), Mass balance of Greenland's three largest outlet glaciers, 2000–2010, *Geophys. Res. Lett.*, *38*, L12501, doi:10.1029/2011GL047565.

Inall, M. E., T. Murray, F. R. Cottier, K. Scharrer, T. J. Boyd, K. J. Heywood, and S. L. Bevan (2014), Oceanic heat delivery via Kangerdlugssuaq Fjord to the south-east Greenland ice sheet, *J. Geophys. Res. Oceans*, *119*, 631–645, doi:10.1002/2013JC009295.

James, T. D., T. Murray, N. Selmes, K. Scharrer, and M. O'Leary (2014), Buoyant flexure and basal crevassing in dynamic mass loss at Helheim Glacier, *Nat. Geosci.*, *7*(8), 593–596, doi:10.1038/ngeo2204.

Jensen, T. S., J. E. Box, and C. S. Hvidberg (2016), A sensitivity study of annual area change for Greenland ice sheet marine terminating outlet glaciers: 1999–2013, *J. Glaciol.*, *62*(231), 72–81, doi:10.1017/jog.2016.12.

Joughin, I. R. (2002), Ice-sheet velocity mapping: A combined interferometric and speckle-tracking approach, *Ann. Glaciol.*, *34*, 195–201.

Joughin, I. R., W. Abdalati, and M. A. Fahnestock (2004), Large fluctuations in speed on Greenland's Jakobshavn Isbrae glacier, *Nature*, *432*(7017), 608–610, doi:10.1038/nature03130.

Joughin, I. R., S. B. Das, M. A. King, B. E. Smith, I. M. Howat, and T. Moon (2008a), Seasonal speedup along the western flank of the Greenland Ice Sheet, *Science*, *320*, 781–783, doi:10.1126/science.1153288.

Joughin, I. R., I. M. Howat, R. B. Alley, G. Ekstrom, M. A. Fahnestock, T. Moon, M. Nettles, M. Truffer, and V. C. Tsai (2008b), Ice-front variation and tidewater behavior on Helheim and Kangerdlugssuaq Glaciers, Greenland, *J. Geophys. Res.*, *113*, F01004, doi:10.1029/2007JF000837.

Joughin, I. R., I. M. Howat, M. Fahnestock, B. E. Smith, W. Krabill, R. B. Alley, H. Stern, and M. Truffer (2008c), Continued evolution of Jakobshavn Isbrae following its rapid speedup, *J. Geophys. Res.*, *113*, F04006, doi:10.1029/2008JF001023.

Joughin, I. R., B. E. Smith, I. M. Howat, T. Scambos, and T. Moon (2010), Greenland flow variability from ice-sheet-wide velocity mapping, *J. Glaciol.*, *56*(197), 415–430.

Joughin, I. R., B. E. Smith, I. M. Howat, D. Floricioiu, R. B. Alley, M. Truffer, and M. A. Fahnestock (2012), Seasonal to decadal scale variations in the surface velocity of Jakobshavn Isbrae, Greenland: Observation and model-based analysis, *J. Geophys. Res.*, *117*, F02030, doi:10.1029/2011JF002110.

Korona, J., E. Berthier, M. Bernard, F. Remy, and E. Thouvenot (2009), SPIRIT. SPOT 5 stereoscopic survey of polar ice: Reference images and topographies during the fourth International Polar Year (2007–2009), *ISPRS J. Photogramm. Remote Sens.*, *64*(2), 204–212, doi:10.1016/j.isprsjprs.2008.10.005.

Krabill, W. B. (2010), *IceBridge ATM L2 Icessn Elevation, Slope, and Roughness, Version 2*, NASA Distributed Active Archive Center, Natl. Snow and Ice Data Cent., Boulder, Colo., doi:10.5067/CPRXXK3F39RV.

Krieger, G., et al. (2013), TanDEM-X: A radar interferometer with two formation-flying satellites, *Acta Astronaut.*, *89*, 83–98, doi:10.1016/j.actaastro.2013.03.008.

Meier, M. F., and A. Post (1987), Fast tidewater glaciers, *J. Geophys. Res.*, *92*, 9051–9058, doi:10.1029/JB092iB09p09051.

Moon, T., and I. R. Joughin (2008), Changes in ice front position on Greenland's outlet glaciers from 1992 to 2007, *J. Geophys. Res.*, *113*, F02022, doi:10.1029/2007JF000927.

Moon, T., I. R. Joughin, B. E. Smith, and I. M. Howat (2012), 21st-century evolution of Greenland outlet glacier velocities, *Science*, *336*, 576–578, doi:10.1126/science.1219985.

Moon, T., I. R. Joughin, B. E. Smith, M. R. Broeke, W. J. Berg, B. Noël, and M. Usher (2014), Distinct patterns of seasonal Greenland glacier velocity, *Geophys. Res. Lett.*, *41*, 7209–7216, doi:10.1002/2014GL061836.

Moon, T., I. R. Joughin, and B. E. Smith (2015), Seasonal to multiyear variability of glacier surface velocity, terminus position, and sea ice/ice melange in northwest Greenland, *J. Geophys. Res. Earth Surf.*, *120*, 818–833, doi:10.1002/2015JF003494.

Morlighem, M., E. Rignot, J. Mouginot, H. Seroussi, and E. Larour (2014), Deeply incised submarine glacial valleys beneath the Greenland ice sheet, *Nat. Geosci.*, *7*, 18–22, doi:10.1038/NGEO2167.

Motyka, R. J., M. Truffer, M. A. Fahnestock, J. Mortensen, S. Rysgaard, and I. M. Howat (2011), Submarine melting of the 1985 Jakobshavn Isbræ floating tongue and the triggering of the current retreat, *J. Geophys. Res.*, *116*, F01007, doi:10.1029/2009JF001632.

Motyka, R. J., et al. (2017), Asynchronous behavior of outlet glaciers feeding Godthåbsfjord (Nuup Kangerlua) and the triggering of Narsap Sermia's retreat in SW Greenland, *J. Glaciol.*, *63*(238), 288–308, doi:10.1017/jog.2016.138.

Murray, T., et al. (2010), Ocean regulation hypothesis for glacier dynamics in southeast Greenland and implications for ice sheet mass changes, *J. Geophys. Res.*, *115*, F03026, doi:10.1029/2009JF001522.

Murray, T., N. Selmes, T. D. James, S. Edwards, I. Martin, T. O'Farrell, R. Aspey, I. Rutt, M. Nettles, and T. Bauge (2015), Dynamics of glacier calving at the ungrounded margin of Helheim Glacier, southeast Greenland, *J. Geophys. Res. Earth Surf.*, *120*, 964–982, doi:10.1002/2015JF003531.

Nettles, M., et al. (2008), Step-wise changes in glacier flow speed coincide with calving and glacial earthquakes at Helheim Glacier, Greenland, *Geophys. Res. Lett.*, *35*, L24503, doi:10.1029/2008GL036127.

Nick, F. M., A. Vieli, I. M. Howat, and I. R. Joughin (2009), Large-scale changes in Greenland outlet glacier dynamics triggered at the terminus, *Nat. Geosci.*, *2*(2), 110–114, doi:10.1038/ngeo394.

Nick, F. M., A. Vieli, M. L. Andersen, I. R. Joughin, A. J. Payne, T. L. Edwards, F. Pattyn, and R. S. W. van de Wal (2013), Future sea-level rise from Greenland's main outlet glaciers in a warming climate, *Nature*, *497*(7448), 235–238, doi:10.1038/nature12068.

Noël, B., W. J. Van De Berg, H. MacHguth, S. Lhermitte, I. Howat, X. Fettweis, and M. R. Van Den Broeke (2016), A daily, 1 km resolution data set of downscaled Greenland ice sheet surface mass balance (1958-2015), *Cryosphere*, *10*(5), 2361–2377, doi:10.5194/tc-10-2361-2016.

Noël, B., W. J. Van De Berg, E. van Meijgaard, P. Kuipers Munneke, R. S. W. Van De Wal, and M. R. Van Den Broeke (2015), Evaluation of the updated regional climate model RACMO2.3: Summer snowfall impact on the Greenland Ice Sheet, *Cryosphere*, *9*(5), 1831–1844, doi:10.5194/tc-9-1831-2015.

O'Leary, M., and P. Christoffersen (2013), Calving on tidewater glaciers amplified by submarine frontal melting, *Cryosphere*, *7*(1), 119–128, doi:10.5194/tc-7-119-2013.

Poinar, K., I. R. Joughin, D. Lilien, L. Brucker, L. M. Kehrl, and S. Nowicki (2017), Drainage of Southeast Greenland firn aquifer water through crevasses to the bed, *Front. Earth Sci.*, *5*, 5, doi:10.3389/FEART.2017.00005.

Reeh, N. (1968), On the calving of ice from floating glaciers, *J. Glaciol.*, *7*(50), 215–232.

Rignot, E., I. Fenty, Y. Xu, C. Cai, I. Velicogna, C. Cofaigh, J. A. Dowdeswell, W. Weinrebe, G. Catania, and D. Duncan (2016), Bathymetry data reveal glaciers vulnerable to ice-ocean interaction in Uummannaq and Vaigat glacial fjords, west Greenland, *Geophys. Res. Lett.*, *43*, 2667–2674, doi:10.1002/2016GL067832.

Rignot, E. J., D. Braaten, S. P. Gogineni, W. B. Krabill, and J. R. McConnell (2004), Rapid ice discharge from southeast Greenland glaciers, *Geophys. Res. Lett.*, *31*, L10401, doi:10.1029/2004GL019474.

Rossi, C., F. Rodriguez Gonzalez, T. Fritz, N. Yague-Martinez, and M. Eineder (2012), TanDEM-X calibrated raw DEM generation, *ISPRS J. Photogramm. Remote Sens.*, *73*, 12–20, doi:10.1016/j.isprsjprs.2012.05.014.

Schild, K. M., and G. S. Hamilton (2013), Seasonal variations of outlet glacier terminus position in Greenland, *J. Glaciol.*, *59*(216), 759–770, doi:10.3189/2013JoG12J238.

Schoof, C. G. (2007), Ice sheet grounding line dynamics: Steady states, stability, and hysteresis, *J. Geophys. Res.*, *112*, F03S28, doi:10.1029/2006JF000664.

Seale, A., P. Christoffersen, R. I. Mugford, and M. O'Leary (2011), Ocean forcing of the Greenland Ice Sheet: Calving fronts and patterns of retreat identified by automatic satellite monitoring of eastern outlet glaciers, *J. Geophys. Res.*, *116*, F03013, doi:10.1029/2010JF001847.

Shapero, D. R., I. R. Joughin, K. Poinar, M. Morlighem, and F. Gillet-Chaulet (2016), Basal resistance for three of the largest Greenland outlet glaciers, *J. Geophys. Res. Earth Surf.*, *121*, 168–180, doi:10.1002/2015JF003643.

Shean, D. E., O. Alexandrov, Z. M. Moratto, B. E. Smith, I. R. Joughin, C. C. Porter, and P. J. Morin (2016), An automated, open-source pipeline for mass production of digital elevation models (DEMs) from very-high-resolution commercial stereo satellite imagery, *ISPRS J. Photogramm. Remote Sens.*, *116*, 101–117, doi:10.1016/j.isprsjprs.2016.03.012.

Shepherd, A. P., et al. (2012), A reconciled estimate of ice-sheet mass balance, *Science*, *338*(6111), 1183–1189, doi:10.1126/science.1228102.

Stearns, L. A., and G. S. Hamilton (2007), Rapid volume loss from two East Greenland outlet glaciers quantified using repeat stereo satellite imagery, *Geophys. Res. Lett.*, *34*, L05503, doi:10.1029/2006GL028982.

Straneo, F., G. S. Hamilton, D. A. Sutherland, L. A. Stearns, F. Davidson, M. O. Hammill, G. B. Stenson, and A. Rosing-Asvid (2010), Rapid circulation of warm subtropical waters in a major glacial fjord in East Greenland, *Nat. Geosci.*, *3*(3), 182–186, doi:10.1038/ngeo764.

Straneo, F., R. G. Curry, D. A. Sutherland, G. S. Hamilton, C. Cenedese, K. Våge, and L. A. Stearns (2011), Impact of fjord dynamics and glacial runoff on the circulation near Helheim Glacier, *Nat. Geosci.*, *4*(5), 322–327, doi:10.1038/ngeo1109.

Sundal, A. V., A. P. Shepherd, M. R. van den Broeke, J. H. van Angelen, N. Gourmelen, and J. Park (2013), Controls on short-term variations in Greenland glacier dynamics, *J. Glaciol.*, *59*(217), 883–892, doi:10.3189/2013JoG13J019.

Truffer, M., and R. Motyka (2016), Where glaciers meet water: Subaqueous melt and its relevance to glaciers in various settings, *Rev. Geophys.*, *54*, 220–239, doi:10.1002/2015RG000494.

van Angelen, J. H., M. R. van den Broeke, B. Wouters, and J. T. M. Lenaerts (2013), Contemporary (1960–2012) evolution of the climate and surface mass balance of the Greenland Ice Sheet, *Surv. Geophys.*, *35*(5), 1155–1174, doi:10.1007/s10712-013-9261-z.

Van Den Broeke, M. R., E. M. Enderlin, I. M. Howat, P. Kuipers Munneke, B. P. Y. Noël, W. Jan Van De Berg, E. van Meijgaard, and B. Wouters (2016), On the recent contribution of the Greenland ice sheet to sea level change, *Cryosphere*, *10*(5), 1933–1946, doi:10.5194/tc-10-1933-2016.

Voytenko, D., A. Stern, D. M. Holland, T. H. Dixon, K. Christianson, and R. T. Walker (2015), Tidally driven ice speed variation at Helheim Glacier, Greenland, observed with terrestrial radar interferometry, *J. Glaciol.*, *61*(226), 301–308, doi:10.3189/2015JoG14J173.

Walter, F., S. O'Neel, D. McNamara, W. T. Pfeffer, J. N. Bassis, and H. A. Fricker (2010), Iceberg calving during transition from grounded to floating ice: Columbia Glacier, Alaska, *Geophys. Res. Lett.*, *37*, L15501, doi:10.1029/2010GL043201.

Zwally, H., R. Schutz, C. Bentley, J. Bufton, T. Herring, J. Minster, J. Spinhirne, and R. Thomas (2003), *GLAS/ICESat L2 Greenland Ice Sheet Altimetry*, Natl. Snow and Ice Data Cent., Boulder, Colo.